

Carboxyl Cellulose Nanocrystal Extracted from Hybrid Poplar Residue

Yu Wu,^a Fei Cao,^a Hua Jiang,^{a,*} and Yang Zhang^b

Ammonium persulfate (APS) oxidation was employed to isolate carboxyl cellulose nanocrystals (CNCs) from hybrid poplar residue. Structure changes resulting from APS oxidation were investigated by Fourier transform infrared (FTIR) spectroscopy and X-ray diffraction (XRD). The further oxidation of the ensuring CNCs with sodium periodate manifested selective oxidation of hydroxyl groups at the C6 position of cellulose into carboxyl groups during APS oxidation. The introduction of active carboxyl groups resulted in lower thermal stability. Transmission electron microscopy (TEM) and width distribution showed that the produced CNCs ranged from 10 nm to 24 nm. Carboxyl CNCs with a yield of 63.2% were isolated *via* APS oxidation, and they were suitable for large-scale CNCs production.

Keywords: Cellulose nanocrystal; Ammonium persulfate; Characterization; Regeoselection

Contact information: a: College of Chemical Engineering, Nanjing Forestry University, Nanjing 210037, China; b: College of Material Science and Engineering, Nanjing Forestry University, Nanjing 210037, China; *Corresponding author: jianghua@njfu.com.cn

INTRODUCTION

Cellulose nanocrystals (CNCs) are a new macromolecular material from biomass that maintains the basic structure and properties of cellulose but also has the characteristics of nanoparticles, such as excellent mechanical strength, renewability, biodegradability, and ease of surface modification (Wegner and Jones 2006; Moon *et al.* 2011). Nowadays, CNCs and their derivatives have received a lot of attention with regards to potential applications in biology, medicine, paper making, and the food industry (Beck-Candanedo *et al.* 2005; Habibi *et al.* 2010; Jackson *et al.* 2011; Pang *et al.* 2015).

Various approaches including mechanical disintegration (Li *et al.* 2012), enzymatic hydrolysis, acid hydrolysis (Lu and Hsieh 2012), and oxidation (Benhamou *et al.* 2014) have been developed to prepare CNCs. Acid hydrolysis (using 64% H₂SO₄) is the most well-known, efficient, and widely used extraction method. Nevertheless, H₂SO₄ hydrolysis faces some problems such as low yield (generally speaking, 33%), waste acid recovery, and corrosion. Recently, ammonium persulfate (APS), a strong oxidizing agent with low long-term toxicity, relative novelty, and low cost, has been applied to prepare CNCs (Leung *et al.* 2011). Nanocellulose was prepared from the oil palm empty fruit bunches using APS oxidation (Goh *et al.* 2016). CNCs were also extracted from bleached bagasse pulp (Du *et al.* 2016) and cotton (Castro-Guerrero *et al.* 2014). However, it has not been reported that CNCs were obtained from hybrid poplar residues using APS oxidation.

Hybrid poplar, a fast-growing tree species abundant in northern China, is typically used for producing paper and plywood. During the processing of hybrid poplar wood, a large amount of residues are generated. These residues are a good source of hemicelluloses.

Additionally, the residues after extracting hemicellulose are abundant in cellulose and are an excellent fiber source for producing CNCs (Jiang *et al.* 2014). Carboxyl groups on the CNCs obtained using APS oxidation provide active sites for the template synthesis of nanoparticles, surface modification, and protein/enzyme immobilization (Wu *et al.* 2017).

The objective of this study was to investigate the feasibility of preparing carboxyl CNCs *via* APS oxidation from hybrid poplar residue (HPR) after the extraction of polymeric hemicelluloses and to study the properties of the CNCs. The obtained CNCs were characterized using structural changes by Fourier transform infrared (FTIR) spectroscopy and X-ray diffraction (XRD), and their thermal properties were characterized with thermogravimetric (TG) analysis. The morphology of the CNCs was investigated by transmission electron microscopy (TEM).

EXPERIMENTAL

Materials

Hybrid poplar, 6 years old, was supplied by Sihong plywood factor in Jiangsu, China. It was ground into small particles, and the 20-mesh to 50-mesh fraction was used. The particulate hybrid poplar was treated using sodium hydroxide solution for the extraction of polymeric hemicelluloses, and the slurry was filtered and washed, and then the residual solid fraction was vacuum dried (Jiang *et al.* 2014). The dry residual solid (HPR) was used as starting material for CNCs in this study. The chemical components were as follows: glucan 60.45%, xylan 4.74%, mannan 1.26%, and Klason lignin 29.85%. Sodium hydroxide (96%) and ammonium persulfate (98%) were purchased from Nanjing chemical reagent Co., Ltd (Nanjing, China). Sodium periodate was purchased from Sinopharm Chemical Reagent Co., Ltd (Shanghai, China).

Preparation of CNCs

HPR (2.5 g), used as the starting material, was added to 250 mL of 1 mol/L APS solution in a 500 mL round bottomed flask. The mixture was stirred with a magnetic stirrer and heated at 65 °C for 14 h to yield a totally white suspension containing the CNCs. The resulting suspension was centrifuged at 12000 rpm for 10 min, and the supernatant was decanted. Deionized water was added, followed by centrifuging again until the solution reached pH 6. All the resulting precipitate was ultrasonicated using the Sonic System Scientz-IIID (NingBo, Zhejiang) with the sonic power of 800 W for 60 s so that a uniform and translucent colloid was formed. The colloidal suspension was lyophilized for CNCs in powder with a Heto PowerDry LL3000 freeze dryer (Thermo, Copenhagen, Denmark).

Sodium Periodate Oxidation of the CNCs

To identify whether the hydroxyl groups at C2 and C3 of cellulose were oxidized by APS, sodium periodate oxidation of the CNCs was performed according to the method described by Chen and van de Ven (2016). Briefly, 0.5 g of CNCs, 1.93 g of NaCl, 0.66 g of NaIO₄, and 32.5 mL of H₂O were mixed and gently stirred for 24 h at room temperature in the dark. When the reaction was finished, excess periodate was decomposed with ethylene glycol, and the product was washed with deionized water until all periodate, salt, and iodate ions were removed. The oxidized CNCs were prepared *via* freeze drying.

Yield of CNCs

A clean crucible was heated in an oven at 105 °C for 2 h and then removed to cool at room temperature and measure its mass (M_1 (g)). The prepared CNCs were put in a crucible, which was heated in an oven at 105 °C for 12 h and then removed to cool at room temperature and measure its mass (M_2 (g)). The CNC yield was calculated with Eq. 1,

$$\text{Yield\%} = \frac{M_2 - M_1}{M_0} \times 100\% \quad (1)$$

where M_0 (g) is the mass of absolutely dry raw material.

Fourier Transform Infrared (FTIR) Spectroscopy

Infrared spectra of the samples were obtained with a VERTEX 80V spectrometer (Bruker, Karlsruhe, Germany). Samples were ground and mixed well with KBr (1 wt.% relative to KBr mass) and pressed into thin pellets prior to analysis. The FTIR analysis was performed in transmittance mode with a wavenumber range of 4000 cm^{-1} to 500 cm^{-1} .

X-ray Diffraction (XRD)

The crystallinities of the raw material and CNCs were evaluated *via* XRD (Rigaku, Tokyo, Japan), which was operated at 40 kV and 30 mA in the scan range of 5 ° to 40 ° and the speed of scan was 5 ° min^{-1} . The crystallinity indexes (CrI) of the cellulose samples were calculated from the diffraction intensity data with Eq. 2 (Segal *et al.* 1959),

$$\text{CrI} = \frac{I_{002} - I_{\text{am}}}{I_{002}} \times 100\% \quad (2)$$

where I_{002} is the overall intensity of the peak at 2θ at 22°, and I_{am} is the intensity of the baseline at 2θ at 18°, which corresponds to the reflection intensity of the amorphous phase.

Thermal Analysis (TG)

Thermogravimetric analysis was carried out with a Pyris 1 TGA (Netzsch, Selb, Germany). The raw material and CNCs were scanned from 35 °C to 600 °C at a heating rate of 10 °C/min. Nitrogen was added at a flow rate of 10 mL/min to avoid sample oxidation.

Transmission Electron Microscopy (TEM)

Morphology and structural investigations were performed using a JSM-7600F transmission electron microscope (Jeol, Tokyo, Japan). A drop of a dilute aqueous suspension (0.1 wt.%) of prepared CNCs was deposited on the surface of a copper grid coated with a thin carbon film. The sample was dried before TEM analysis which was carried out with an accelerating voltage of 100 kV to 120 kV.

Zeta Potential

The zeta potential values of the CNCs were measured with a Zeta-sizer Nano (Malvern, England). The CNCs suspension (3 wt.%) was diluted in water at the ratio of 1:1000 (v/v) and ultrasonicated for 30 s in an ultrasonic bath. The refractive index of the water was 1.470, and the analysis temperature was 25 °C.

RESULTS AND DISCUSSION

Visual Images

Figure 1a shows the image of raw material containing APS solution before any reaction had taken place. The prepared CNCs were ultrasonicated to form a homogeneous hydrogel, as shown in Fig. 1b. As shown in Fig. 1a and Fig. 1b, the color of the raw material changed from yellow to white, indicating that the raw material had been oxidized. This phenomenon occurred because when the solution containing APS was heated, the formation of free radicals was induced ($S_2O_8^{2-} + \text{heat} \rightarrow 2SO_4^{\cdot-}$). Under acidic conditions, hydrogen peroxide was also formed ($S_2O_8^{2-} + 2H_2O \rightarrow 2HSO_4^+ + H_2O_2$) (Hsu *et al.* 2002). Both free radicals and hydrogen peroxide are capable of penetrating the amorphous domains and removing the disordered cellulose to form highly crystalline CNCs; meanwhile, free radical and hydrogen peroxide can decolorize materials without any catalysts or mechanical treatments (Leung *et al.* 2011). The prepared CNCs powder after freeze drying is shown in Fig. 1c. The obtained CNCs had a yield of 63.2% (calculated by Eq. 1), which was much higher than what is obtained during the conventional H_2SO_4 hydrolysis (25 to 35%) (Goh *et al.* 2016). These results suggest that large-scale CNCs production might be obtained from HPR *via* APS oxidation.

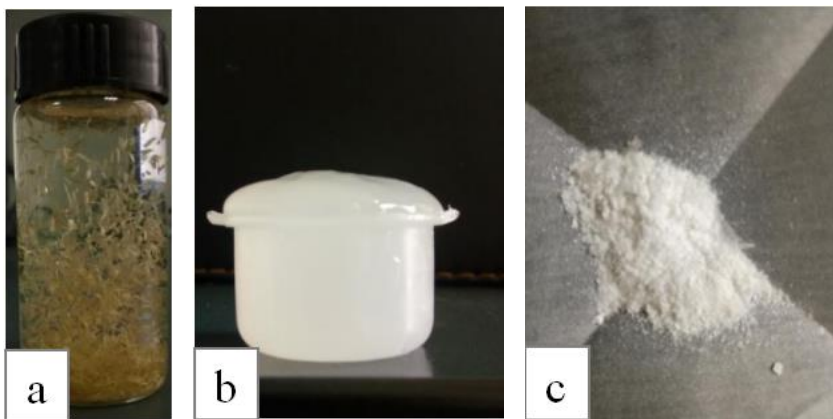


Fig. 1. (a) Raw material containing APS solution; (b) CNCs after ultrasonication; (c) CNCs after freeze-drying

FTIR Characterization

The FTIR spectra of the raw material and CNCs are presented in Fig. 2a. For raw material, the band observed at 3411 cm^{-1} is attributed to O-H vibration, which mainly resulted from hydrogen bonds in cellulose I. The bands at 2918 cm^{-1} and 1434 cm^{-1} are associated with C-H and C-H₂ stretching vibrations, respectively (Hua *et al.* 1993; Saito *et al.* 2007), and the band at 1635 cm^{-1} is related to the absorbed water (Marchessault and Liang 1960). The CNCs exhibited similar infrared peaks. However, a band at 1735 cm^{-1} was present; it is related to the C=O stretching vibration. The presence of C=O suggested that the hydroxyl groups of the CNCs had been oxidized successfully after APS oxidation (Oh *et al.* 2005). In addition, the peak at approximately 1506 cm^{-1} signaled the presence of the lignin, as it represented the C=C stretching vibration in the aromatic ring of lignin (Sun *et al.* 2000; Chen *et al.* 2011). The absence of this characteristic peak after APS oxidation indicated that the lignin was effectively removed.

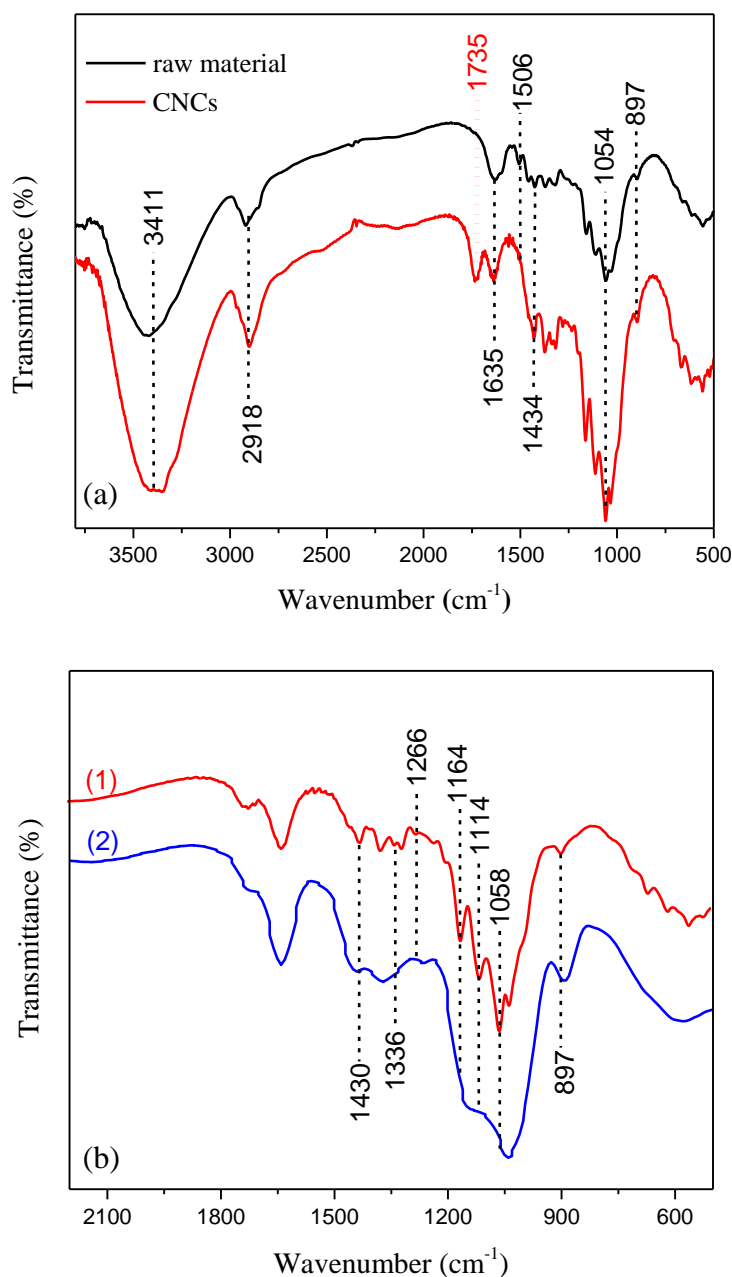


Fig. 2. FTIR spectra of (a) the raw material and CNCs and (b) CNCs (1) and CNCs further oxidized by sodium periodate for 24 h (2)

To further investigate whether the hydroxyl groups at C6 of CNCs were selectively oxidized into carboxyl groups during APS oxidation, sodium periodate oxidation of the CNCs was performed. Figure 2b depicts the FTIR spectra of the CNCs (1) and the CNCs further oxidized by sodium periodate for 24 h (2). The CNCs displayed absorption bands at 1336 cm⁻¹ and 1266 cm⁻¹, which are associated with the vibrations of hydroxy groups at C2 and C3 of cellulose (Carrillo *et al.* 2004), and the bands at 1058 cm⁻¹, 1114 cm⁻¹, and 1164 cm⁻¹ are related to the C-O-O pyranose ring stretching vibration, the C-C ring stretching vibration, and the C-O-C glycosidic ether band, respectively.

Periodate oxidation is a highly selective stereospecific reaction that only breaks the C2-C3 bond in the glucose repeat units of cellulose, forming two vicinal aldehyde groups (Chen and van de Ven 2016). Compared with (1) and (2) of Fig. 2b, the adsorption bands at 1430 cm^{-1} , 1336 cm^{-1} , 1266 cm^{-1} , 1164 cm^{-1} , 1114 cm^{-1} , and 1058 cm^{-1} became weaker after periodate oxidation. Namely, the adsorption peaks of the hydroxyl groups at C2 and C3 weakened or even disappeared, which indicated that the hydroxyl groups at C2 and C3 remained integrated during the APS oxidation. Therefore, the hydroxyl group at C6 of cellulose was selectively oxidized into carboxyl form after APS oxidation.

XRD Analysis

X-ray diffraction studies were conducted to evaluate the crystalline behaviors of the raw material and CNCs. Celluloses are semicrystalline biopolymers with both crystalline and amorphous domains. The difference between chemical treatments on the crystallinity index of the cellulose can be determined and compared from the XRD results. As shown in Fig. 3, both samples exhibited obvious diffraction peaks at 15.4° , 16.4° , 22.8° , and 34.7° , which are attributed to the crystal planes of -110, 110, 200, and 400 in cellulose, respectively (Wada *et al.* 2004; Saito *et al.* 2007). These findings suggested that APS oxidation did not change the crystalline structure of native cellulose. The X-ray diffraction patterns of the CNCs confirmed that the integrity of the crystalline structure remained during the course of APS oxidation (Leung *et al.* 2011). The crystallinity index of the raw material and the CNCs were 52.6% and 86.8%, respectively, as calculated from Eq. 2. Hence, highly crystalline CNCs could be produced *via* APS oxidation because the majority of the amorphous region in cellulose was removed.

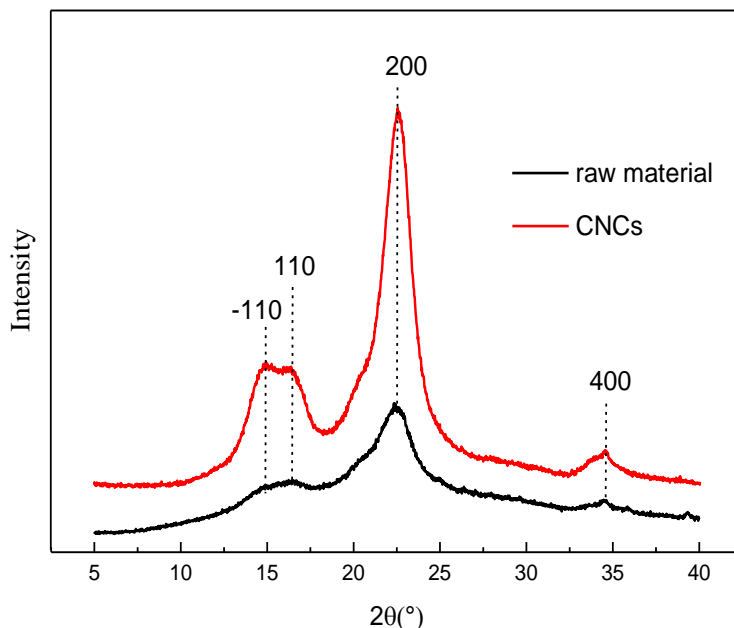


Fig. 3. X-ray diffraction spectra of the raw material and CNCs

TG Analysis

Figure 4 illustrates the thermogravimetric (TG) and derived curves (DTG) of the raw material and CNCs, respectively. The initial weight loss in the range of 30°C to 120°C observed for both samples was attributed to the removal of water absorbed within cellulose (Chen *et al.* 2011).

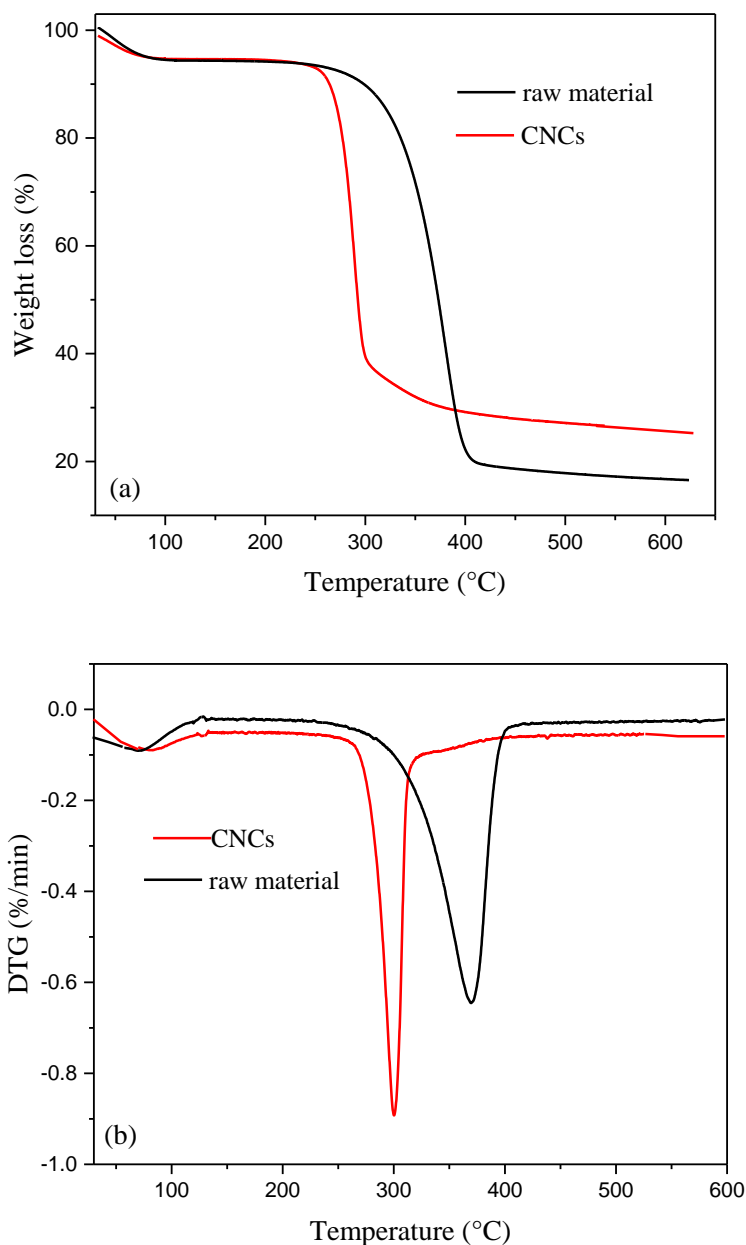


Fig. 4. TG (a) and DTG (b) curves of CNC and raw material

As shown in the DTG curves for the CNCs, weight loss started at around 265 °C, which was related to the initial thermal decomposition, followed by a drastic weight loss at 265 °C to 290 °C, and then a slow weight loss up to 330 °C. Compared to the CNCs, the weight loss of the raw material was slower in the range of 310 °C to 370 °C, and the onset degradation temperature of the CNCs (265 °C) was lower than that of the raw material (310 °C), which was mainly due to the introduction of active carboxyl groups, the small particle size, and the high specific surface area of the CNCs after oxidation, which increased the exposed surface area with heating and decreased the thermostability (Popescu *et al.* 2011; Jiang and Hsieh 2013). Fortunately, the CNCs prepared *via* APS oxidation were stable when the temperature was less than 260 °C. This is important for thermoplastic

applications of cellulose nanoparticles because the processing temperature is often above 200 °C. The CNCs obtained from sulfuric acid hydrolysis had lower thermal stability, ranging from 150 °C to 200 °C due to the presence of sulfate groups (Cheng *et al.* 2014). Furthermore, the percentage of the CNCs that remained as char residue (27%) was higher than that of the raw material (16%) at the end of the test. This result occurred because the highly crystalline nature (cellulose crystal) of the CNCs increased the proportion of carbon. Therefore, the formation of char residue increased as carbon content increased (George *et al.* 2011).

TEM Analysis

As shown in Fig. 5a, the morphological features of CNCs whisker were observed *via* TEM. The image expressed that the distribution of CNCs isolated from hybrid poplar was uniform and they dispersed well in solution with a relative interparticle distance, which was mainly due to the presence of charge resulting in electrostatic repulsive force. These charges were mainly derived from the dissociation of sodium carboxylate of the CNCs, and the existence of the carboxyl groups was confirmed with FTIR. It is reported (Mirhosseini *et al.* 2008) that if the absolute value of suspension was higher than 25 mV, then the suspension was not vulnerable to aggregation. The zeta potential of the CNCs suspension (0.1 wt.%, p H 7) was about -49 mV, which indicated the CNCs suspension was stable.

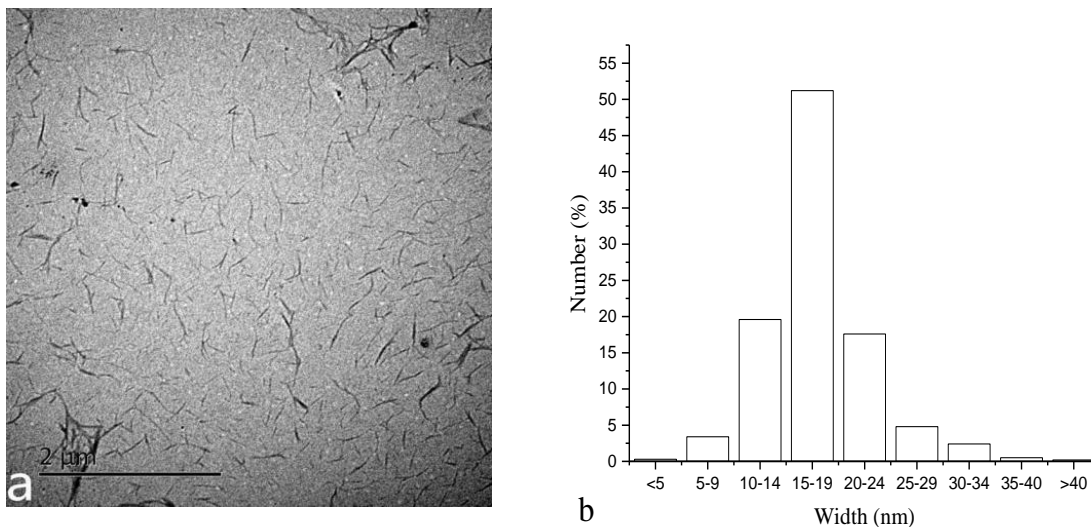


Fig. 5. Transmission electron microscopy image (a) and width distribution (b) of the CNCs

To examine the size distribution of the CNCs, the widths of 150 individual CNCs were measured from TEM images (5 images were used to measure) using a Gatan DigitalMicrograph®. The width was defined as the largest dimension measured across the CNCs. The results are displayed in Fig. 5b, which showed that the width of the CNCs had a range of distribution within the range 5 nm to 40 nm in width and the main distribution of the width is from 10 nm to 24 nm. Therefore, thin and short whisker of carboxyl CNCs were prepared after APS oxidation, which is beneficial in supporting the active sites for the synthesis of nanoparticles and surface modification.

CONCLUSIONS

1. HPR was utilized as a source of cellulose for producing carboxyl CNCs *via* APS oxidation. Fourier transform infrared spectroscopy confirmed the introduction of carboxyl groups onto the surface of CNCs, and lignin was effectively removed.
2. The further oxidation of the CNCs with sodium periodate manifested hydroxyl groups at C6 of cellulose were selectively oxidized into carboxyl groups during APS oxidation. X-ray diffraction and TG revealed that carboxylated CNCs had a higher crystallinity (86.8%) than that of raw material (52.6%) but had lower thermal stability.
3. TEM displayed a main distribution in the range of 10 nm to 24 nm and the final yield of the CNCs extracted from HPR by APS oxidation was approximately 63.2%.

ACKNOWLEDGMENTS

This work was financially supported by the Special Fund for Forest Scientific Research in the Public Welfare (201504603) and the Priority Academic Program Development (PAPD) of Jiangsu Higher Education Institutions of China.

REFERENCES CITED

- Beck-Candanedo, S., Roman, M., and Gray, D. G. (2005). "Effect of reaction conditions on the properties and behavior of wood cellulose nanocrystal suspensions," *Biomacromolecules* 6(2), 1048-1054. DOI: 10.1021/bm049300p
- Benhamou, K., Dufresne, A., Magnin, A., Mortha, G., and Kaddami, H. (2014). "Control of size and viscoelastic properties of nanofibrillated cellulose from palm tree by varying the TEMPO-mediated oxidation time," *Carbohydrate Polymers* 99, 74-83. DOI: 10.1016/j.carbpol.2013.08.032
- Castro-Guerrero, C. F., and Gray, D. G. (2014). "Chiral nematic phase formation by aqueous suspensions of cellulose nanocrystals prepared by oxidation with ammonium persulfate," *Cellulose* 21(4), 2567-2577. DOI: 10.1007/s10570-014-0308-1
- Chen, D., and van de Ven, T. G. M. (2016). "Morphological changes of sterically stabilized nanocrystalline cellulose after periodate oxidation," *Cellulose* 23(2), 1051-1059. DOI: 10.1007/s10570-016-0862-9
- Chen, W., Yu, H., Liu, Y., Chen, P., Zhang, M., and Hai, Y. (2011). "Individualization of cellulose nanofibers from wood using high-intensity ultrasonication combined with chemical pretreatments," *Carbohydrate Polymers* 83(4), 1804-1811. DOI: 10.1016/j.carbpol.2010.10.040
- Cheng, M., Qin, Z., Liu, Y., Qin, Y., Li, T., Chen, L., and Zhu, M. (2014). "Efficient extraction of carboxylated spherical cellulose nanocrystals with narrow distribution through hydrolysis of lyocell fibers by using ammonium persulfate as an oxidant," *Journal of Materials Chemistry A* 2, 251-258. DOI: 10.1039/c3ta13653a
- Du, C., Liu, M., and Li, B. (2016). "Cellulose nanocrystals prepared by persulfate one-step oxidation of bleached bagasse pulp," *BioResources* 11, 4017-4024. DOI:

- 10.15376/biores.11.2.4017-4024
- George, J., Ramava, K. V., Bawa, A. S., and Siddaramaiah (2011). "Bacterial cellulose nanocrystals exhibiting high thermal stability and their polymer nanocomposites," *International Journal of Biological Macromolecules* 48(1), 50-57. DOI: 10.1016/j.ijbiomac.2010.09.013
- Goh, K. Y., Ching, Y. C., Chuah, C. H., Abdullah, L. C., and Liou, N. (2016). "Individualization of microfibrillated celluloses from oil palm empty fruit bunch: Comparative studies between acid hydrolysis and ammonium persulfate oxidation," *Cellulose* 23(1), 379-390. DOI: 10.1007/s10570-015-0812-y
- Guerrero, C. F. C. G. (2013). "Preparation and properties of cellulose nanocrystals prepared by ammonium persulfate oxidation of cotton and wood fibers," in: 245th National Meeting of the American-Chemical-Society (ACS), Vol. 245. New Orleans.
- Habibi, Y., Lucia, L. A., and Rojas, O. J. (2010). "Cellulose nanocrystals: Chemistry, self-assembly, and applications," *Chemical Reviews* 110(6), 3479-3500. DOI: 10.1021/cr900339w
- Hsu, S.-C., Don, T.-M., and Chiu, W.-Y. (2002). "Free radical degradation of chitosan with potassium persulfate," *Polymer Degradation and Stability* 75(1), 73-83. DOI: 10.1016/S0141-3910(01)00205-1
- Hua, X., Kaliaguine, S., Kokta, B. V., and Adnot, A. (1993). "Surface analysis of explosion pulps by ESCA," *Wood Science and Technology* 28, 1-8.
- Jackson, J. K., Letchford, K., Wasserman, B. Z., Ye, L., and Hamad, W. Y. (2011). "The use of nanocrystalline cellulose for the binding and controlled release of drugs," *International Journal of Nanomedicine* 6, 321-330. DOI: 10.2147/IJN.S16749
- Jiang, F. and Hsieh, Y. L. (2013). "Chemically and mechanically isolated nanocellulose and their self-assembled structures," *Carbohydrate Polymers* 95(1), 32-40. DOI: 10.1016/j.carbpol.2013.02.022
- Jiang, H., Chen, Q., Ge, J., and Zhang, Y. (2014). "Efficient extraction and characterization of polymeric hemicelluloses from hybrid poplar," *Carbohydrate Polymers* 101, 1005-1012. DOI: 10.1016/j.carbpol.2013.10.030
- Leung, A. C. W., Hrapovic, S., Lam, E., Liu, Y., Male, K. B., Mahmoud, K. A., and Luong, J. H. T. (2011). "Characteristics and properties of carboxylated cellulose nanocrystals prepared from a novel one-step procedure," *Small* 7(3), 302-305. DOI: 10.1002/sml.201001715
- Li, J., Wei, X., Wang, Q., Chen, J., Chang, G., Kong, L., Su, J., and Liu, Y. (2012). "Homogeneous isolation of nanocellulose from sugarcane bagasse by high pressure homogenization," *Carbohydrate Polymers* 90(4), 1609-1613. DOI: 10.1016/j.carbpol.2012.07.038
- Lu, P., and Hsieh, Y. (2012). "Preparation and characterization of cellulose nanocrystals from rice straw," *Carbohydrate Polymers* 87(1), 564-573. DOI: 10.1016/j.carbpol.2011.08.022
- Marchessault, R. H. and Liang, C. Y. (1960). "Infrared spectra of crystalline polysaccharides. 3. Mercerized cellulose," *Journal of Polymer Science* 43(141), 71-84. DOI: 10.1002/pol.1960.1204314107
- Mirhosseini, H., Tan, C. P., Hamid, N. S. A., and Yusof, S. (2008). "Effect of arabic gum, xanthan gum and orange oil contents on zeta-potential, conductivity, stability, size index and pH of orange beverage emulsion," *Colloids and Surfaces A: Physicochemical and Engineering Aspects* 315(1-3), 47-56. DOI:

10.1016/j.colsurfa.2007.07.007

- Moon, R. J., Martini, A., Nairn, J., Simonsen, J., and Youngblood, J. (2011). "Cellulose nanomaterials review: Structure, properties and nanocomposites," *Chemical Society Reviews* 40(7), 3941-3994. DOI: 10.1039/c0cs00108b
- Oh, S. Y., Yoo, D. I., Shin, Y., Kim, H. C., Kim, H. Y., Chung, Y. S., Park, W. H., and Youk, J. H. (2005). "Crystalline structure analysis of cellulose treated with sodium hydroxide and carbon dioxide by means of X-ray diffraction and FTIR spectroscopy," *Carbohydrate Research* 340(15), 2376-2391. DOI: 10.1016/j.carres.2005.08.007
- Pang, Z., Sun, X., Wu, X., Nie, Y., and Liu, Z. (2015). "Fabrication and application of carbon nanotubes/cellulose composite paper," *Vacuum* 122(A), 135-142. DOI: 10.1016/j.vacuum.2015.09.020
- Saito, T., Kimura, S., Nishiyama, Y., and Isogai, A. (2007). "Cellulose nanofibers prepared by TEMPO-mediated oxidation of native cellulose," *Biomacromolecules* 8(8), 2485-2491. DOI: 10.1021/bm0703970
- Segal, L., Creely, J., Martin, A., and Conrad, C. (1959). "An empirical method for estimating the degree of crystallinity of native cellulose using the X-ray diffractometer," *Textile Research Journal* 29, 786-794. DOI: 10.1177/004051755902901003
- Sun, R. C., Tomkinson, J., Wang, Y. X., and Xiao, B. (2000). "Physico-chemical and structural characterization of hemicelluloses from wheat straw by alkaline peroxide extraction," *Polymer* 41(7), 2647-2656. DOI: 10.1016/S0032-3861(99)00436-X
- Wada, M., Heux, L., and Sugiyama, J. (2004). "Polymorphism of cellulose I family: Reinvestigation of cellulose IV," *Biomacromolecules* 5(4), 1385-1391. DOI: 10.1021/bm0345357
- Wegner, T. H., and Jones, P. E. (2006). "Advancing cellulose-based nanotechnology," *Cellulose* 13(2), 115-118. DOI: 10.1007/s10570-006-9056-1
- Wu, Y., Cao, F., Jiang, H., and Zhang, Y. (2017). "Preparation and characterization of aminosilane-functionalized cellulose nanocrystal aerogel," *Materials Research Express* 4(8), DOI: 10.1088/2053-1591/aa8067

Article submitted: July 23, 2017; Peer review completed: September 24, 2017; Revised version received and accepted: October 2, 2017; Published: October 6, 2017.

DOI: 10.15376/biores.12.4.8775-8785